metals

MDPI

Article

Investigating the Effects and Mechanisms of Thermal–Vibration-Coupled Stress Relief Treatment on Residual Stress in SiC/Al Composites

Bianhong Li [1,2,*], Wu Ouyang [1] and Yushuang Dong [1]

[1] College of Technology, Beijing Forestry University, No. 35 Qinghua East Road, Beijing 100091, China; yangwu@bjfu.edu.cn (W.O.); dt7220295@bjfu.edu.cn (Y.D.)
[2] Key Laboratory of National Forestry and Grassland Administration on Forestry Equipment and Automation, Beijing Forestry University, Beijing 100091, China
* Correspondence: libianhong@bjfu.edu.cn

Abstract: Aluminum matrix composites reinforced with particles (PRAMCs) frequently develop considerable residual stresses post-quenching, which can negatively affect fatigue life and dimensional accuracy. Traditional stress relief methods for aluminum alloys are only partially effective. This study examined thermal stress relief (TSR), vibratory stress relief (VSR), and a combined thermal–vibratory stress relief (TVSR) approach for SiC/Al composites. All treatments proved successful in diminishing residual stresses, with the most significant reduction along the direction of peak dynamic stress. Additionally, this study analyzed micro-residual stresses via a macro–micro-residual stress finite element model to understand differences in stress relief outcomes. Optimizing the TVSR process could be key to more effectively reducing residual stresses in SiC/Al composites.

Keywords: thermal–vibration-coupled stress relief; macro–micro-stress; metallic composites; residual stress; simulation and modeling

Citation: Li, B.; Ouyang, W.; Dong, Y. Investigating the Effects and Mechanisms of Thermal–Vibration-Coupled Stress Relief Treatment on Residual Stress in SiC/Al Composites. *Metals* **2024**, *14*, 1195. https://doi.org/10.3390/met14101195

Academic Editor: Frank Czerwinski

Received: 10 September 2024
Revised: 11 October 2024
Accepted: 16 October 2024
Published: 21 October 2024

1. Introduction

The fabrication of particle-reinforced aluminum matrix composites (PRAMCs) leads to significant residual stress due to the mismatch in thermal expansion and the elastic modulus between the matrix and reinforcement phases [1]. While residual compressive stress from processes like shot peening can enhance fatigue life, the majority of residual stresses are detrimental [2,3]. An uneven stress distribution during composite preparation can weaken mechanical properties [4], cause damage [5], reduce fatigue life, and affect dimensional stability [6–8]. Techniques such as thermal stress relief (TSR), vibratory stress relief (VSR), and thermal–vibratory-coupled stress relief (TVSR) are well-established for metallic materials.

TSR is the process of inducing stress relaxation or creep in materials through prolonged high, low, or high/low temperature cycling, accompanied by changes in mechanical properties such as the elastic modulus and yield limit [9]. It converts the elastic strain energy inside the material into plastic strain energy, thereby reducing residual stress [10,11]. The advantages of this type of method are a good overall stress regulation effect and uniform stress distribution after regulation, while the disadvantages are high energy consumption and low efficiency [12]. TSR not only reduces residual stress, but also affects the microstructure and mechanical properties of materials. Research has shown that after heat aging treatment at 340 °C for 1 h, the deformation caused by the residual stress of 6061 aluminum alloy parts is reduced by 60%, but the tensile strength is reduced by 20% [13]. The use of multi-stage segmented TSR can significantly reduce the residual stress formed during the quenching of the Al-Zn-Mg-Cu alloy, with a reduction of 2.9 times that of traditional TSR [14]. Heating at 760 °C and holding for 45 min during TSR can significantly eliminate the residual stress generated in TC4 titanium alloy during friction stir welding, and

the stress peak can be reduced from 350 MPa to 40 MPa [15]. For 2014 aluminum-based Al_2O_3 composite materials, TSR at 250 °C for 10 h can reduce residual stress from 43 MPa to 18 MPa and increase yield limit from 203 MPa to 272 MPa [16]. With the increase in heating temperature during TSR, the dynamic recrystallization grain size of short carbon fiber-reinforced magnesium-based composites decreases, and residual stress decreases to some extent; after heating at 610 °C for another 30 min, the tensile strength of the composite material also significantly increases [17].

VSR is the process of applying static or cyclic force loads to a material, causing it to reach its yield limit as a whole or locally, resulting in plastic deformation and stress release [18]. The advantages of this type of method are high efficiency, lower energy consumption, a flexible form, and enhanced mechanical properties [19]. The disadvantages are a limited application scope and a poor overall stress control effect [20]. VSR has a significant effect on eliminating residual stress in 7075-T651 aluminum alloy specimens. Compared with the control group, the average residual stress of the 7075-T651 aluminum alloy specimens decreased by 84.82%, 85.27%, 77.84%, 75.82%, 79.39%, and 75.30% after six different amplitude VSR treatments [21]. After hot VSR, the residual stress distribution of AZ31 magnesium alloy becomes more uniform. As the vibration time increases, the compressive residual stress first increases and then decreases [22]. After VSR treatment, the residual stress of the Al-Mg-Si-Cu alloy tends to be uniform, with a reduction of 52.6% in compressive residual stress and less than 10% in tensile residual stress [23]. With the increase in extrusion times, the grain size of short carbon fiber-reinforced magnesium-based composite materials begins to decrease, and the yield strength and ultimate tensile strength of the composite materials are increased by 50.15% and 63.60%, respectively, compared to extruded magnesium alloys [24].

TVSR is an emerging residual stress control method that combines VSR in thermal loads and TSR in force loads, complementing each other's strengths and weaknesses. Existing research mainly focuses on metal. Research has shown that the maximum residual stress of 7075 aluminum alloy treated with TVSR is higher than those of TSR and VSR, respectively [25,26]. After VSR, TSR, and TVSR treatments, the maximum residual stress of both 2219 aluminum alloy welded specimens and a 2219 aluminum alloy ring decreased, respectively, and the stress control effect of TVSR was significantly better than that of TSR and VSR [27–29]. In the treatment of Ti6Al4V titanium alloys, it has been shown that the efficiency and relief rate of TVSR are both better than TSR and VSR [30]. For the treatment of an Al-Cu-Mg alloy plate, the results show that TVSR treatment has a stress relief rate 81.7% higher than that of TSR [31].

Research on residual stress elimination in PRAMCs is scarce.

The addition of SiC particles to Al alloys modifies residual stress development during heat treatment [32,33]. While studies have examined the impact of preparation and heat treatment on PRAMCs' mechanical properties and microstructure, as well as the formation and evolution of residual stresses in composites with varying particle volumes and sizes [34], few have addressed the stress release mechanisms. This study targets the residual stress relief in SiC/Al composites using TSR, VSR, and TVSR treatments, based on Al alloy processes. It aims to assess the effectiveness of these treatments on PRAMCs fabricated by powder metallurgy (PM), offering insights for stress regulation in PRAMCs.

2. Materials and Methods

2.1. Specimen and Experiment Process

The research conducted in this study focuses on the analysis of 20 vol.% SiC/Al-Cu-Mg composite plates, which have been fabricated using the powder metallurgy (PM) process. These composite plates feature SiC particles with an average size of 5 μm, dispersed within an aluminum alloy matrix that contains copper and magnesium as secondary phases. The precise dimensions of the composite plates are detailed in Figure 1a. The chemical composition for the matrix—the Al-Cu-Mg alloy—is shown in Table 1.

Table 1. The chemical composition for the matrix Al-Cu-Mg alloy (mass fraction/%).

Element	Cu	Mg	Si	Fe	Zn	Cu	Al
Content	3.2–4.4	1.0–1.9	0.25	0.2	0.1	3.2–4.4	Surplus

Powder Metallurgy Process: The Powder Metallurgy Process is a manufacturing technique that involves blending fine powdered materials, pressing them into a desired shape, and then sintering the compacted material at high temperatures to create a solid product. This method is particularly suitable for producing composites with a uniform distribution of reinforcement particles like SiC within a metal matrix.

The specific Powder Metallurgy Process: The SiC particles, with an average size of 5 μm, act as a reinforcement, while the Al-Cu-Mg alloy powder forms the matrix. The types of powders are mixtures of chemical elements. A tumbling process is used in dry mixing for obtaining the uniform distribution of the reinforcing powder—SiC. The blended powder mixture is then compacted into a desired shape using a cold isostatic pressing technique. This step ensures a uniform distribution of SiC particles within the Al matrix. Sintering temperatures: lower temperature range: 525 °C to 550 °C for a longer sintering time to promote solid-state sintering without excessive grain growth. Higher temperature range: up to 575 °C to 600 °C for a shorter sintering time, but with a greater risk of grain growth and a potential for SiC damage if not carefully controlled.

Heat Treatment: The specimens in this study were subjected to a heat treatment process that began with solid solution treatment at a temperature of 490 °C for a duration of 60 min. This step allows for the dissolution of secondary phases into the aluminum matrix, enhancing the material's properties. Following the solid solution treatment, the specimens were quenched in water at room temperature to rapidly cool them, which helps to retain the solutes in a supersaturated solid solution and to achieve a desired microstructure.

Initial State (process #0): The specimens underwent a heat treatment at 490 °C for 60 min for solid solution treatment, followed by quenching in water at room temperature which represented the initial state of the material without any subsequent stress relief procedures. This initial state was labeled as process #0. The specimens in this condition were used as a baseline to compare the effects of various stress relief treatments on the residual stress levels within the composite material.

Stress Relief Treatments: Different stress relief treatments were applied to subsequent specimens, as outlined in Figure 1b. These treatments are aimed at reducing the residual stresses induced by the quenching process, which can affect the material's mechanical properties and dimensional stability.

Specimen #1 (TSR): This specimen underwent thermal stress relief (TSR) at 175 °C. TSR involves heating the material to a specific temperature below the recrystallization temperature and then cooling it slowly to allow the internal stresses to relax.

Specimens #2–#3 (TVSR): These specimens were treated with thermal–vibratory-coupled stress relief (TVSR). TVSR combines the thermal and vibratory methods to achieve stress relief. The specimens are heated and simultaneously subjected to vibratory motion, which can enhance the stress relaxation process.

Specimen #4 (VSR): This specimen received vibratory stress relief (VSR), a method that involves applying vibrational energy to the material to help release internal stresses without the use of heat.

The application of these various stress relief treatments allows for a comparative analysis of their effectiveness in reducing residual stresses in the SiC/Al-Cu-Mg composites, providing valuable insights into the optimization of manufacturing processes for such materials.

2.2. TVSR Equipment and Flow

TVSR integrates VSR and TSR methods, applying a vibratory load at an optimal temperature to leverage the combined effects of thermal and mechanical forces for stress elimination. These aging processes are crucial steps in the heat treatment of aluminum al-

loys, particularly for precipitation-hardened alloys like Al-Cu-Mg systems. After a solution treatment, which involves heating the alloy to a high temperature to dissolve all the solute elements into the matrix, the alloy is quenched to rapidly cool it and retain the solutes in a supersaturated state. This supersaturated state is unstable and eventually leads to the precipitation of solute atoms from the matrix, forming discrete particles within the material. This precipitation process is controlled by aging, which involves heating the alloy to a lower temperature for a specific period of time. During aging, the solute atoms diffuse and gather to form precipitates, which act as obstacles to dislocation movement, thus strengthening the material. The size, distribution, and type of precipitates formed during aging determine the resulting mechanical properties of the alloy. The TVSR setup used in this research was developed by Beihang University (No. 37 Xueyuan Road, Haidian District, Beijing). Figure 1c,d depict the TVSR experiment clamp and on-site setup, as well as the operating principles.

The vibration system's frequency and the specimen's placement on the platform were established using ANSYS modal analysis. The finite element model of modal analysis treats the exciter as a concentrated particle; the modeling of four supports connects the vibration table to the ground, using four sets of spring elements in three directions. Both the workpiece and the vibration table are modeled using the 3D solid element Solid185. The finite element simulation model in Figure 1e reveals a first-order modal frequency of 60.03 Hz, characteristic of a bending vibration mode. The second-order modal frequency, however, was beyond the exciter's operational range, as seen in Figure 1g. The vibration platform's first modal frequency, measured through the hammer modal method, aligned with the simulation at 60.8 Hz. Consequently, the exciter speed was fixed at 3600 rpm, with the sample placement shown in Figure 1f. Following evidence that TSR and TVSR at 175 °C are effective for stress relief in 2XXX series Al alloys [6,9], this study adopted the same temperature for experimentation.

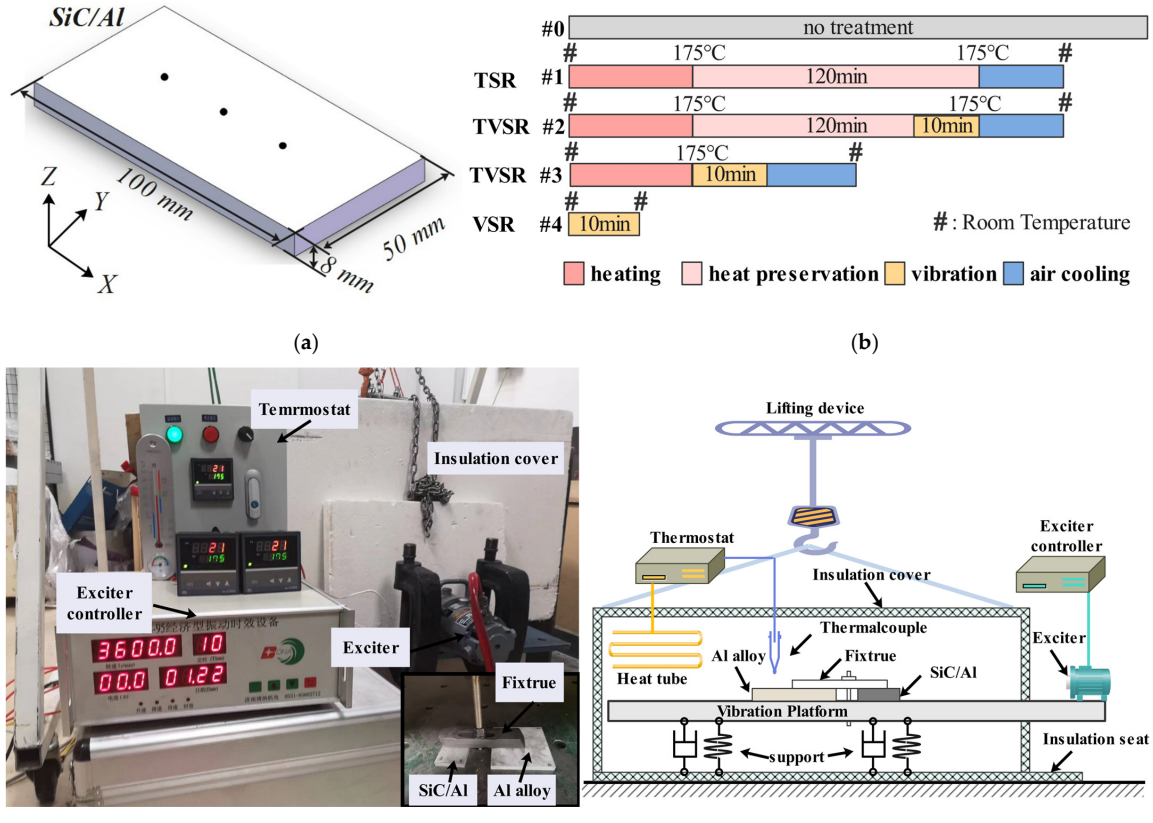

Figure 1. *Cont.*

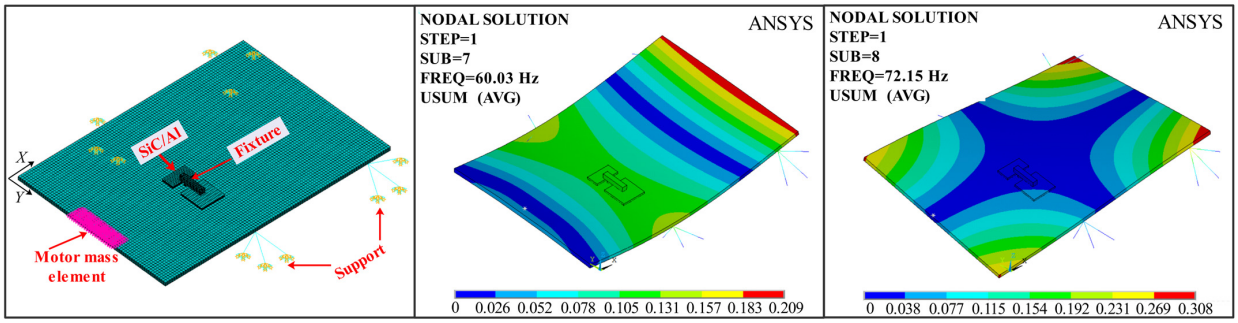

(**e**) (**f**) (**g**)

Figure 1. Illustrations of various aspects of the study: (**a**) the SiC/Al composite specimen; (**b**) specific stress relief treatment parameters; (**c**) the TVSR experimental setup; (**d**) the TVSR working principle; (**e**) the finite element (FE) simulation model; (**f**) first-order modal deformation; and (**g**) second-order modal deformation.

In traditional VSR, the exciter is installed on the test sample, and then a certain frequency of vibration is applied and maintained for a certain period of time. This type of VSR is called direct VSR; for smaller samples, they are generally installed on a vibration platform, with the sample and exciter mounted on the vibration platform, and then vibrated at a certain frequency for a period of time. This vibration is indirectly applied to the test sample, referred to as indirect VSR or platform VSR. Based on previous research, for platform VSR, the excitation frequency is generally selected as the resonance frequency of the vibration platform, and the vibration time is generally 10 min.

Implementation of TVSR: Initially, the furnace was set to a target temperature of 175 °C using the temperature controller. A thermocouple monitored the air temperature near the fixed workpiece. Once the target temperature was reached, it was maintained while the vibration exciter operated for 10 min. After vibration, the specimen was kept in the furnace for a specified holding time before the heating system was turned off. The specimen was then cooled to room temperature (20 °C) in the air. The holding times during the TVSR experiments were either 0 or 110 min.

The implementation of the thermal–vibration stress relief (TVSR) process involves a series of carefully controlled steps to ensure the effective reduction in residual stress in a SiC/Al composite material. Below is an expanded description of the TVSR process:

Preparation of the Furnace: The furnace is initially prepared for the TVSR process by setting the temperature controller to a target temperature of 175 °C. This temperature is chosen based on the material's thermal properties and the desired level of stress relief. It is crucial to select a temperature that is high enough to facilitate stress relaxation without causing any thermal damage to the composite material.

Monitoring Temperature: A thermocouple is used to monitor the air temperature in close proximity to the workpiece, which is securely fixed within the furnace. The thermocouple provides real-time feedback to the temperature controller, ensuring that the furnace maintains the desired temperature with high precision.

Achieving and Maintaining Target Temperature: Once the furnace reaches the target temperature of 175 °C, the heating system is regulated to maintain this temperature throughout the process. Stability in temperature is essential for the effectiveness of the stress relief treatment.

Vibration Application: With the target temperature achieved and maintained, the vibration exciter is activated and operates for a duration of 10 min. The vibration exciter induces controlled vibrations into the workpiece, which help to further relieve the residual stresses within the material. The specific frequency and amplitude of the vibrations are selected based on the material's response and previous experimental data.

Holding Time: After the 10 min vibration period, the specimen is kept in the furnace for a specified holding time. This holding time allows the material to undergo additional stress relaxation at the elevated temperature. In the TVSR experiments, two different holding times were used: 0 min and 110 min. The 0 min holding time serves as a control to assess the effectiveness of the vibration alone, while the 110 min holding time provides an extended period for thermal stress relief in conjunction with the vibration.

Cooling Process: Following the vibration and holding time, the heating system in the furnace is turned off, and the specimen is allowed to cool down to room temperature, which is typically set at 20 °C. The cooling process is conducted in the ambient air, and it is important to ensure a controlled cooling rate to prevent the re-introduction of stress into the material.

Considerations: Throughout the TVSR process, it is essential to control all variables to ensure consistent and repeatable results. This includes the heating rate, temperature uniformity, vibration parameters, and cooling rate. Additionally, the process must be carefully documented to allow for analysis and optimization of the stress relief outcomes.

The TVSR process combines the benefits of thermal and vibration stress relief, and by varying the holding times, researchers can study the impact of each component on the overall effectiveness of the stress reduction. The results of these experiments can then be used to optimize the TVSR process for the SiC/Al composite material or other materials with similar properties.

3. Results and Discussion

3.1. Redisual Stress Results of SiC/Al Composites

After the experiment is completed, the residual stress is measured using the blind hole method. The definition of its measuring points and directions is shown in Figure 1a, where the measuring positions are P1, P2, and P3 from left to right, with P2 being the center position of the sample. The residual stress results after vibration aging are shown in Figure 2.

Figure 2 provides a detailed illustration of the effects of various stress relief treatments on the SiC/Al composite material. The SiC/Al composite, after undergoing the quenching process, shows a considerable amount of compressive stress on its surface. This stress is particularly pronounced in the Y-direction relative to the X-direction, indicating anisotropic stress distribution.

To alleviate this stress, three different treatments were applied: thermal stress relief (TSR), vibration stress relief (VSR), and thermal–vibration stress relief (TVSR). Each of these methods were effective in reducing the surface stress of the SiC/Al composite, although the degree of stress reduction was notably less than that observed in the 2024Al alloy, as previously reported in reference [31].

When examining the directional stress relief, the TVSR process was particularly effective in reducing stress in the X-direction, much more so than in the Y-direction. This difference can be attributed to the characteristics of the TVSR process itself. During TVSR, the vibration platform operates at its first-order modal frequency, which corresponds to a first-order bending vibration mode. This bending mode generates more dynamic stress in the X-direction. As a result, the residual stress in the X-direction, which is coupled with the dynamic stress, is more substantial and thus more easily relaxed during the treatment process, in agreement with findings from earlier studies [31].

In contrast, the TSR and VSR processes show less pronounced differences in directional stress reduction. The TSR process, which relies solely on thermal means to relieve stress, might not be as effective in addressing the anisotropic stress distribution due to the uniform application of heat. Similarly, the VSR process, which uses only vibration, may not target the X-directional stress as effectively as the combined TVSR method.

When analyzing the von Mises stress, which is a measure of the equivalent stress and is used to predict material failure, the TSR treatment proved to be the most effective in stress reduction, followed by the TVSR process (specifically configurations #2 and #3), with the VSR method being the least effective. This hierarchy of effectiveness can be related to the mechanisms by which each treatment interacts with the residual stress within the material.

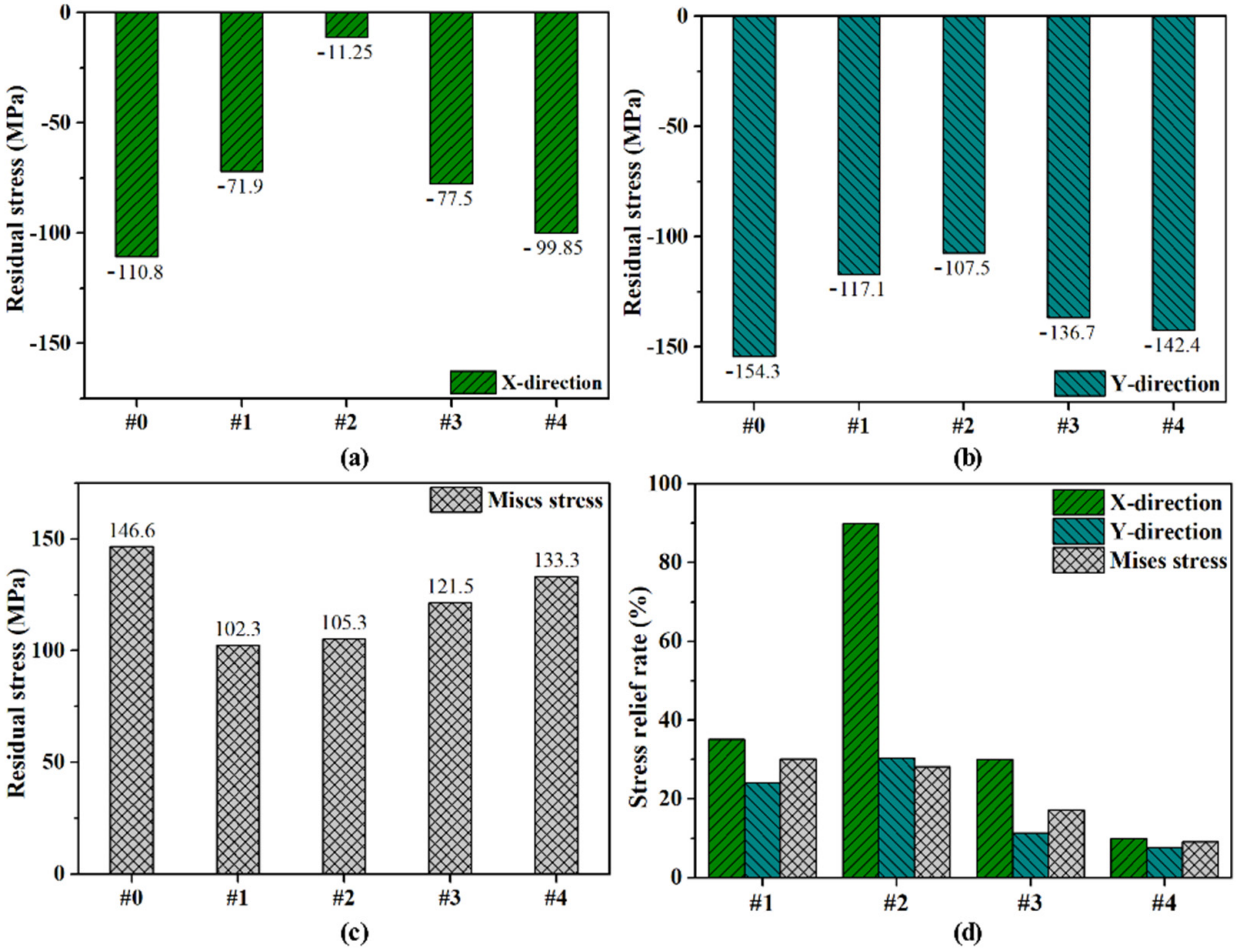

Figure 2. Presentation of the residual stress outcomes in the SiC/Al composites, both pre- and post-stress relief treatments, including the following: (**a**) X-direction stress, (**b**) Y-direction stress, (**c**) von Mises stress, and (**d**) stress relief rate.

The shape of the sample is also a critical factor influencing the stress relief process. The geometry of the sample can lead to variations in how the TSR stress relief is applied, potentially causing uneven stress reduction across the material. The bending vibration mode employed in the TVSR process takes advantage of the sample's shape to target the X-directional stress more effectively, resulting in a more pronounced reduction in stress in that direction.

In summary, the stress relief treatments applied to the SiC/Al composite material yield varying degrees of effectiveness, with the TVSR process demonstrating a unique ability to target and reduce stress in the X-direction due to its vibration characteristics. These findings underscore the importance of selecting the appropriate stress relief method based on the material properties and the desired outcome.

3.2. Stress Evolution Mechanism

A comprehensive macro–micro finite element (FE) model was developed to investigate the quenching process of 20 volume percent SiC/Al composites, as depicted in Figure 3a. This model is a sophisticated numerical tool designed to provide insights into the stress distributions at both macroscopic and microscopic levels during the quenching of the composite material.

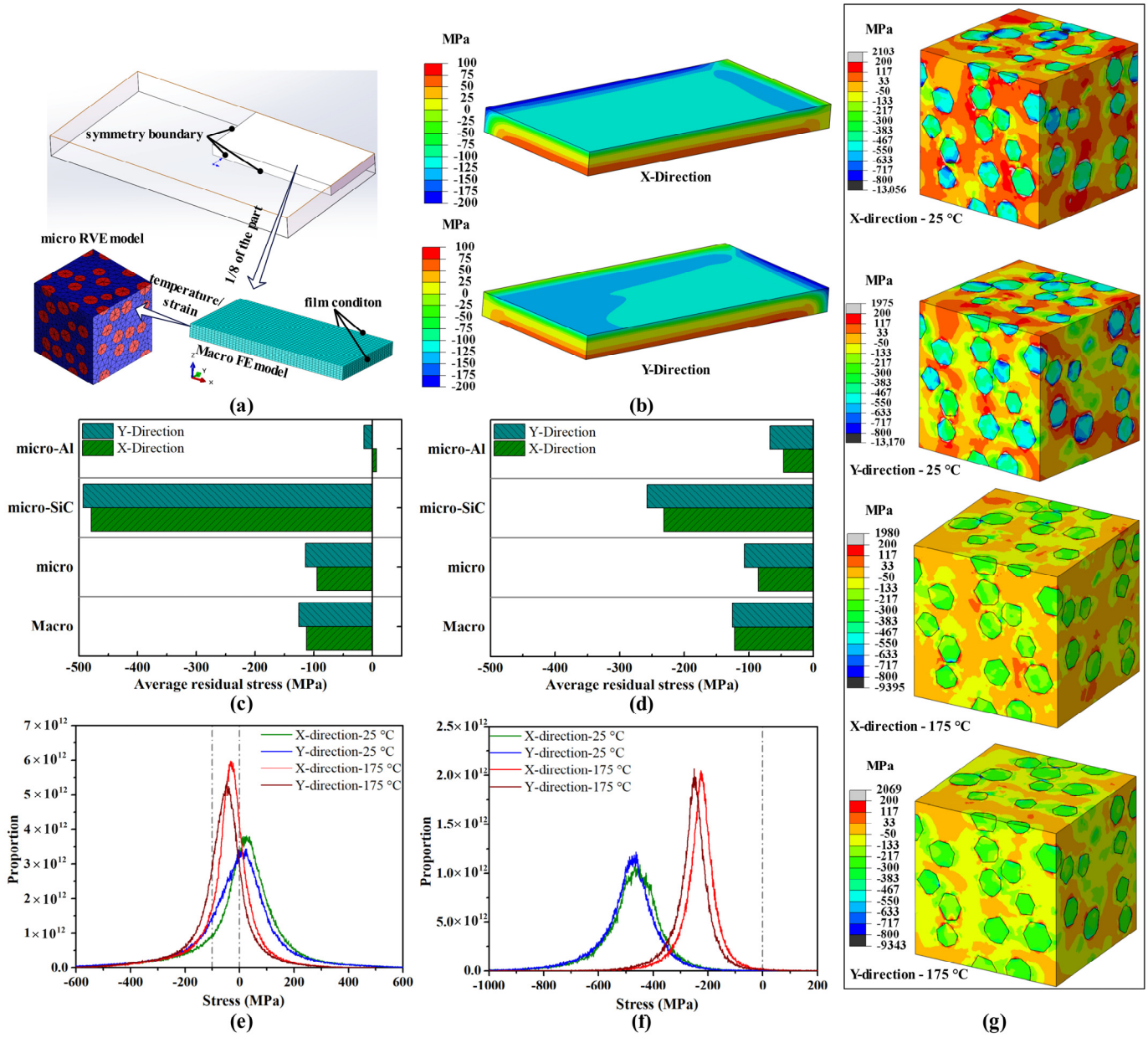

Figure 3. Depictions of the following: (**a**) the macro–micro FE model and boundary condition; (**b**) macroscopic residual stress post-quenching; (**c**) microscopic average residual stress post-quenching; (**d**) microscopic average residual stress at 175 °C; (**e**) micro-residual stress distribution in the Al matrix; (**f**) micro-residual stress distribution within the SiC inclusion; and (**g**) contours of microscopic residual stress under varying conditions.

3.2.1. Model Structure:

Macroscopic Level: At the macroscopic level, the model simulates the overall behavior of the 20 vol.% SiC/Al composite during the quenching process. It focuses on the macro residual stresses that are generated as the material is rapidly cooled from an initial temperature of 490 °C to a final temperature of 25 °C. This part of the model captures the thermal gradients and phase transformations that occur during cooling, which are the primary drivers of residual stress development in the composite.

Microscopic Level: The microscopic level of the model delves deeper into the material's structure to calculate the stresses that develop at the individual reinforcement (SiC) and matrix (Al alloy) levels. This level of detail is crucial for understanding the stress distribution

within the composite, as the SiC particles and the Al matrix have different thermal expansion coefficients and mechanical properties, leading to complex stress interactions [35].

3.2.2. Material Properties:

SiC and Al Alloy Properties: The material properties for the SiC particles and the Al alloy matrix were sourced from reference [36]. These properties include thermal conductivity, specific heat (Table 2), density (Table 3), thermal expansion coefficient (Table 4), and mechanical properties, such as Young's modulus and Poisson's ratio (Tables 5–7).

Table 2. Material thermal conductivity and specific heat capacity.

Material	Temperature (°C)	25	100	200
Al	Thermal conductivity ($W \cdot m^{-1} \cdot K^{-1}$)	179.5	208.3	227.8
	Specific heat capacity ($J \cdot kg^{-1} \cdot K^{-1}$)	1152	1285	1341
SiC	Thermal conductivity ($W \cdot m^{-1} \cdot K^{-1}$)	108.8	69.9	39.8
	Specific heat capacity ($J \cdot kg^{-1} \cdot K^{-1}$)	709	724	873
SiC/Al	Thermal conductivity ($W \cdot m^{-1} \cdot K^{-1}$)	163.1	173.4	177.8
	Specific heat capacity ($J \cdot kg^{-1} \cdot K^{-1}$)	1047	1152	1230

Table 3. Composite materials and their component densities.

Material	Al	SiC	SiC/Al
Density (kg/m^3)	2750	3250	2850

Table 4. Average coefficient of thermal expansion of materials (1×10^{-6}/K).

Temperature (°C)	Al	SiC/Al	SiC
100	23.09	16.63	3.60
200	24.13	18.30	4.58
300	25.18	18.95	5.32
400	26.28	19.66	5.84
500	27.27	22.10	6.13

Table 5. Al mechanical properties.

Temperature (°C)	Yield Strength (Mpa)	Tensile Strength (Mpa)	Elongation Rate (%)
25	301.8	436.3	19.01
100	288.6	415.0	43.04
200	238.2	294.8	7.88
300	-	101.3	0.12
500	4.7	4.8	66

Table 6. SiC/Al mechanical properties.

Temperature (°C)	Yield Strength (Mpa)	Tensile Strength (Mpa)	Elongation Rate (%)
25	289.5	304.4	0.49
100	291.6	309.0	0.13
200	271.4	290.0	0.29
300	133.3	134.4	0.26
500	9.2	9.9	1.11

Table 7. Composite materials, elastic modulus, and Poisson's ratio of each phase.

Material	Al	SiC	SiC/Al	
Temperature (°C)	**Elastic Modulus (GPa)**		**Elastic Modulus (GPa)**	**Poisson's Ratio**
25	70.13	420	97.86	0.27537
100	67.52		94.68	0.27545
200	63.63		89.89	0.27556
300	59.29		84.46	0.27568
400	54.49		77.47	0.27582
500	49.24		69.62	0.27759

SiC/Al Composite Properties: To model the behavior of the SiC/Al composite as a whole, the material properties were obtained through a homogenization method, as described in reference [36]. Homogenization is a technique used to derive effective material properties for composite materials by averaging the properties of the constituent phases, taking into account their volume fractions and spatial distributions.

3.2.3. Model Implementation and Analysis:

The macro–micro FE model was implemented using specialized software (ABAQUS secondary development language Python 2023 version) capable of handling both thermal and mechanical simulations. The model was constructed with appropriate boundary conditions to mimic the quenching process, including the application of heat transfer coefficients to simulate the cooling medium (such as water or air) and constraints to represent the physical constraints on the material during quenching.

The simulation was conducted in several steps:

1. Initialization: The initial temperature distribution was set across the composite, reflecting the pre-quenching temperature of 490 °C.
2. Quenching Simulation: The model was then used to simulate the cooling process, capturing the temperature changes and the resulting stress developments at both macroscopic and microscopic levels.
3. Stress Analysis: After the quenching simulation, the model provided data on the residual stresses at both levels. These data were analyzed to understand the stress distribution and the interactions between the SiC particles and the Al matrix.
4. Validation: The model's results were compared with experimental data to validate its accuracy and reliability. Adjustments to the model parameters were made as necessary to improve the model's predictive capabilities.

By integrating both macroscopic and microscopic analyses, this macro–micro FE model offers a powerful tool for understanding the complex stress mechanisms in SiC/Al composites during the quenching process, which is essential for optimizing manufacturing processes and enhancing the material's performance.

The quenching process of the 20 vol.% SiC/Al composite material resulted in a distinct stress distribution across the specimen's cross-section, as illustrated in Figure 3b. This stress distribution is characterized by compressive stress on the surface and tensile stress in the core region of the specimen, a common occurrence in materials subjected to rapid cooling due to the differential contraction of the surface and the core.

Surface Stress State: At the surface center of the specimen, the compressive stress was measured to be −112 MPa in the X-direction and −125 MPa in the Y-direction. These values indicate a higher magnitude of compressive stress in the Y-direction compared to the X-direction, which aligns with findings reported in the literature [36]. This directional difference in the residual stress is primarily influenced by the dimensions of the specimen, with the stress distribution being anisotropic due to the shape and cooling conditions of the material.

Consistency of Simulation Results: The finite element (FE) simulation results from both the macroscopic and microscopic models demonstrated a high degree of consistency, as evidenced by the comparison shown in Figure 3c. This consistency validates the accuracy of the macro–micro FE model in predicting the stress distribution within the composite material.

Stress in the Al Alloy Matrix and SiC Reinforcement: After the quenching process, the average stress in the Al alloy matrix was observed to be close to zero, suggesting that the matrix undergoes minimal residual stress after cooling. In contrast, the SiC reinforcement phase experienced an average stress of approximately −480 MPa, indicating a significant amount of compressive stress within the ceramic particles. This discrepancy in stress between the matrix and the reinforcement is due to the different coefficients of thermal expansion and mechanical properties of the two phases.

Microscopic Stress Distribution: The distribution and contour map of microscopic stress after quenching are detailed in Figure 3e–g. These figures reveal that only a small number of regions within the composite exhibited high stress levels. These high-stress areas were predominantly found in the vicinity of the matrix surrounding the SiC particles, particularly in regions where the particles were closely spaced. The stress concentration in these areas can be attributed to the geometric constraints imposed by the closely packed particles, which restrict the matrix's ability to contract during cooling, leading to higher stress levels. Even when SiC particle agglomeration occurs, this could extremely influence the residual stress distribution and the effectiveness of stress relief treatments.

The detailed stress distribution provided by the macro–micro FE model is crucial for understanding the mechanical behavior of the SiC/Al composite material. This insight can inform the design and processing of the material to minimize the risk of stress-induced failures and to enhance the overall performance and reliability of the composite in various applications.

As the temperature of the 20 vol.% SiC/Al composite material increases from room temperature (25 °C) to the aging temperature of 175 °C, the material's stress state undergoes distinct changes at both the macroscopic and microscopic levels. The following details the observed stress variations and the underlying mechanisms:

Macroscopic Stress Stability: At the macroscopic level, the stress within the composite shows minimal change with the increase in temperature. This stability suggests that the overall stress state of the composite is relatively insensitive to temperature variations within the range studied.

Microscopic Stress Variations: In contrast to the macroscopic stress, the microscopic stress experiences significant alterations. The average stress in the Al matrix increases to approximately −50 MPa, indicating an increase in compressive stress as the temperature rises. Conversely, the average stress in the SiC reinforcement phase decreases to around −240 MPa, showing a reduction in compressive stress within the ceramic particles.

Stress Dispersion: The temperature increase also leads to a decrease in the dispersion of stress within the composite. This reduction in stress variability suggests that the stress distribution becomes more uniform as the material is heated, which could be attributed to the thermal expansion of both phases and the resulting stress relaxation.

Thermal Expansion Mismatch: The differences in the thermal expansion coefficient and the elastic modulus between the Al matrix and the SiC reinforcement phases are the primary drivers of the observed stress changes [37]. The thermal expansion coefficient of the Al alloy is several times greater than that of SiC [38]. As the material is heated, the Al matrix expands more than the SiC reinforcement, leading to a mismatch in thermal expansion between the two phases.

Stress Development During Heating: Typically, during the heating process, the greater thermal expansion of the Al matrix relative to the SiC reinforcement results in tensile stress developing in the matrix and compressive stress in the reinforcement. This is because the matrix's expansion is constrained by the less expansive reinforcement, creating internal stresses.

Microscopic vs. Macroscopic Stress: Despite the microscopic thermal mismatch stresses, these do not translate into significant changes in the macroscopic stress state of the composite. The simulation results confirm that while the microscopic stress levels and distribution are affected by the temperature increase, the overall macroscopic stress remains relatively unchanged.

Conclusion: The simulation findings underscore the complex interplay between the matrix and reinforcement phases in SiC/Al composites under thermal loading. The microscopic stress variations highlight the importance of considering thermal expansion mismatches when designing and analyzing the performance of composite materials. Understanding these stress mechanisms is crucial for optimizing the processing and performance of SiC/Al composites, particularly in applications where temperature fluctuations are a concern.

The decrease in stress during TSR treatment is mainly due to stress relaxation at elevated temperatures. This process can be roughly modeled by equation [35].

$$\dot{\varepsilon}_c = A\sigma^n t^m \exp\left(-\frac{Q}{RT}\right) \quad (1)$$

where, A, n, m, Q, and R are the material constants, σ is the stress, t is the time, and T is the relaxation temperature.

In SiC/Al composites, the SiC phase remains stable during aging with no stress relaxation [39], meaning stress reduction is mainly due to the Al matrix relaxation. Post-quenching, the Al matrix experiences low compressive stress, leading to a lower relaxation rate during TSR than in pure Al alloys, aligning with previous findings [6]. The VSR process's effectiveness in SiC/Al composites is also affected by the microstress state. Harmonic response analysis shows that TVSR treatment induces higher dynamic stress in the X-direction and less in the Y-direction [31]. The combination of Al matrix stress and dynamic stress increases stress in the X-direction, enhancing relaxation. Thus, the X-direction's relaxation rate exceeds the Y-direction's during TVSR, suggesting that TVSR is more effective in directions with higher dynamic stress. Adopting bidirectional vibration stress relief could potentially further increase the stress relief rate with TVSR.

4. Conclusions and Expectation

4.1. Conclusions

This study examined thermal stress relief (TSR), vibratory stress relief (VSR), and a combined thermal–vibratory stress relief (TVSR) approach for SiC/Al composites. The conclusion is as follows:

(1) Post-quenching, SiC/Al composites feature macroscopic compressive stress, with the Al matrix's average stress near zero at the microscopic level and the SiC phase under significant compressive stress. Raising the temperature from 25 °C to 175 °C increases the Al matrix's compressive stress and reduces it in the SiC phase.

(2) TSR, VSR, and TVSR treatments all reduce residual stress in SiC/Al composites, though less effectively than in pure Al alloys due to the lower micro-residual stress in the matrix. In terms of von Mises stress relief, the effectiveness order is TSR > TVSR (treatments #2, #3) > VSR.

(3) TVSR is most effective in the X-direction, as the combination of the Al matrix's microstress and dynamic stress raises the stress level, enhancing relaxation. This suggests TVSR's high potential for residual stress elimination in SiC/Al composites.

Based on the findings and discussion presented in the manuscript, here are some suggestions for further research and potential modifications:

4.2. Further Research

The Effect of SiC Particle Size and Volume Fraction: Investigate how the size and volume fraction of SiC particles influence the residual stress distribution and the effectiveness

of the stress relief treatments. This could provide valuable insights into optimizing the composite design for specific applications.

Microstructure and Property Changes: Analyze the microstructure of the SiC/Al composites after different stress relief treatments to understand the impact on the material properties. This would help in assessing the trade-off between stress relief and the potential degradation of mechanical properties.

Long-Term Stability: Study the long-term stability of the residual stress relief in SiC/Al composites under different environmental conditions. This is crucial for ensuring the reliability and durability of the material in practical applications.

4.3. Potential Modifications

Comparison with Other Stress Relief Methods: Include a comparison with other stress relief methods like shot peening or laser peening to provide a comprehensive assessment of the TVSR method's effectiveness and applicability.

Finite Element Model Refinement: Refine the finite element model by incorporating more detailed material properties and considering additional factors like temperature gradients and phase transformations. This would improve the accuracy and reliability of the model predictions.

Experimental Parameters Optimization: Conduct a systematic study to optimize the TVSR process parameters, including temperature, vibration frequency, amplitude, and holding time, for maximum stress relief and minimal impact on material properties.

By addressing these suggestions, researchers can gain a deeper understanding of the residual stress relief mechanisms in SiC/Al composites and optimize the TVSR method for improved material performance and reliability.

Author Contributions: Conceptualization: B.L. and W.O.; methodology: B.L.; software: Y.D.; validation: B.L., W.O. and Y.D.; formal Analysis: B.L. and W.O.; investigation: W.O. and Y.D.; resources: B.L., W.O. and Y.D.; data curation: B.L., W.O. and Y.D.; writing—original draft preparation: B.L. and W.O.; writing—review and editing: B.L., W.O. and Y.D.; visualization: B.L.; supervision: B.L.; project administration: B.L.; funding acquisition: B.L. All authors have read and agreed to the published version of the manuscript.

Funding: This work was financially supported by the National Natural Science Foundation of China (No. 52375140) and the Fundamental Research Funds for the Central Universities (No. BLX202230).

Data Availability Statement: The original contributions presented in the study are included in the article, further inquiries can be directed to the corresponding author.

Conflicts of Interest: The authors declare no conflict of interest.

References

1. Miller, K.; Wang, X. Impact of Residual Stresses on Mechanical Properties of Particle-Reinforced Metal-Matrix Composites. *J. Compos. Mater.* **2023**, *57*, 1675–1690.
2. Sun, R.; Cao, Z.; Zhang, Y.; Zhang, H.; Yu, Y. Laser Shock Peening of Sicp/2009Al Composites: Microstructural Evolution, Residual Stress and Fatigue Behavior. *Materials* **2021**, *14*, 1082. [CrossRef] [PubMed]
3. Hu, Y.; Cheng, H.; Yu, J.; Yao, Z. An Experimental Study on Crack Closure Induced by Laser Peening in Pre-Cracked Aluminum Alloy 2024-T351 and Fatigue Life Extension. *Int. J. Fatigue* **2020**, *130*, 105231–105232. [CrossRef]
4. Zhang, Q.; Yang, M.; Liu, P. Impact of Interphase Damage and Residual Stresses on the Mechanical Performance of Particle Reinforced Metal-Matrix Composites. *Mater. Manuf. Process.* **2023**, *38*, 1274–1286.
5. Wang, H.; Zhang, T.; Li, J. Micromechanical Analysis of Debonding in Fiber-Reinforced Composites Due to Residual Curing Stresses. *Mater. Manuf. Process.* **2023**, *38*, 749–759.
6. Zhou, L.; Zhang, X.; Chen, Y. Influence of Heat Treatment on Stress Relief and Dimensional Stability in SiC Particle Reinforced Aluminum Composites. *Mater. Manuf. Process.* **2024**, *39*, 156–167.
7. Gao, H.; Zhang, Y.; Wu, Q.; Li, B. Investigation on Influences of Initial Residual Stress on Thin-Walled Part Machining Deformation Based on A Semi-Analytical Model. *J. Mater. Process. Technol.* **2018**, *262*, 437–448. [CrossRef]
8. Li, B.; Deng, H.; Hui, D.; Hu, Z.; Zhang, W. A Semi-Analytical Model for Predicting the Machining Deformation of Thin-Walled Parts Considering Machining-Induced and Blank Initial Residual Stress. *Int. J. Adv. Manuf. Technol.* **2020**, *110*, 139–161. [CrossRef]

9. Liu, Y.; Zhang, R.; Chen, Z. Mechanical Properties and Heat Treatment of SAE 4130 Steel Plates. *Mater. Manuf. Process.* **2023**, *38*, 450–460.
10. Song, H.; Gao, H.; Wu, Q.; Zhang, Y. Residual Stress Relief Mechanisms of 2219 Al–Cu Alloy by Thermal Stress Relief Method. *Rev. Adv. Mater. Sci.* **2022**, *61*, 102–116. [CrossRef]
11. Yang, J.; Bu, K.; Zhou, Y.; Song, K.; Song, Y.; Huang, T.; Peng, X.; Liu, H.; Du, Y. Influence of Short-Time Annealing on the Evolution of The Microstructure, Mechanical Properties and Residual Stress of the C19400 Alloy Strips. *J. Alloys Compd.* **2023**, *941*, 168705. [CrossRef]
12. Wu, Q.; Wu, J.; Zhang, Y.D.; Gao, H.; Hui, D. Analysis and Homogenization of Residual Stress in Aerospace Ring Rolling Process of 2219 Aluminum Alloy Using Thermal Stress Relief Method. *Int. J. Mech. Sci.* **2019**, *157*, 111–118. [CrossRef]
13. Wang, X.; Liu, Y.; Zhang, J. Effects of Heat Treatment and Aging on Microstructural Evolution and Phase Transformation in Ti-6Al-4V Alloy Wire. *Mater. Manuf. Process.* **2023**, *38*, 1053–1065.
14. Sun, Y.; Jiang, F.; Hui, Z.; Jian, S.; Yuan, W. Residual Stress Relief in Al–Zn–Mg–Cu Alloy by A New Multistage Interrupted Artificial Aging Treatment. *Mater. Des.* **2016**, *92*, 281–287. [CrossRef]
15. Hönnige, J.R.; Colegrove, P.A.; Ahmad, B.; Fitzpatrick, M.E.; Ganguly, S.; Lee, T.L.; Williams, S.W. Residual Stress and Texture Control In Ti-6Al-4V Wire + Arc Additively Manufactured Intersections by Stress Relief and Rolling. *Mater. Des.* **2018**, *150*, 193–205. [CrossRef]
16. Fernandez, R.; Cabeza, S.; Mishurova, T.; Fernandez-Castrillo, P.; Gonzalez-Doncel, G.; Bruno, G. Residual Stress and Yield Strength Evolution with Annealing Treatments in an Age-Hardenable Aluminum Alloy Matrix Composite. *Mater. Sci. Eng. A* **2018**, *731*, 344–350. [CrossRef]
17. Yang, Z.; Xu, H.; Wang, Y.; Hu, M.; Ji, Z. Influence of Reheating Temperature on the Microstructures and Tensile Properties of A Short-Carbon-Fiber-Reinforced Magnesium Matrix Composite. *Mater. Res. Express* **2019**, *6*, 106547.
18. Peng, N.; Zhan, L.; Song, Z.; Zhu, W.; Xu, Y.; Ma, B.; Zeng, Q.; Chen, K.; Lao, S.; Zheng, Q. Strengthening Mechanism of 2219 Al-Cu Alloy by Room-Temperature Random Vibration. *J. Alloys Compd.* **2023**, *934*, 167878. [CrossRef]
19. Xue, N.; Wu, Q.; Zhang, Y.; Li, B.; Zhang, Y.; Yang, S.; Zhu, Y.; Guo, J.; Gao, H. Review on Research Progress and Comparison of Different Residual Stress Strengthening Methods for Titanium Alloys. *Eng. Fail. Anal.* **2023**, *144*, 106937. [CrossRef]
20. Ebrahimi, S.; Farahani, M.; Akbari, D. The Influences of the Cyclic Force Magnitude and Frequency on the Effectiveness of the Vibratory Stress Relief Process on A Butt Welded Connection. *Int. J. Adv. Manuf. Technol.* **2019**, *102*, 2147–2158. [CrossRef]
21. Gao, H.; Zhang, Y.; Wu, Q.; Song, J.; Wen, K. Fatigue Life of 7075-T651 Aluminium Alloy Treated with Vibratory Stress Relief. *Int. J. Fatigue* **2017**, *108*, 62–67. [CrossRef]
22. Wang, J.; Hsieh, C.; Lai, H.; Kuo, C.; Wu, T.; Wu, W. The Relationships Between Residual Stress Relaxation and Texture Development in Az31 Mg Alloys Via the Vibratory Stress Relief Technique. *Mater. Charact.* **2015**, *99*, 248–253. [CrossRef]
23. Albedah, A.; Khan, S.; Benyahia, F.; Bouiadjra, B. Effect of Load Amplitude Change on the Fatigue Life of Cracked Al Plate Repaired with Composite Patch. *Int. J. Fatigue* **2016**, *88*, 1–9. [CrossRef]
24. Yang, Z.; Xu, H.; Wang, Y.; Hu, M.; Ji, Z. Microstructures and Mechanical Properties of SCF/AZ31B Composites Fabricated by Multi-Times Hot-Extrusion. *Results Phys.* **2018**, *12*, 888–895. [CrossRef]
25. Gao, H.; Wu, S.; Wu, Q.; Li, B.; Mo, S. Experimental and Simulation Investigation on Thermal-Vibratory Stress Relief Process for 7075 Aluminium Alloy. *Mater. Des.* **2020**, *195*, 108954. [CrossRef]
26. Xu, Y.; Shi, Z.; Li, B.; Zhang, Z. Effects of TVSR Process on the Dimensional Stability and Residual Stress of 7075 Aluminum Alloy Parts. *Rev. Adv. Mater. Sci.* **2021**, *60*, 631–642. [CrossRef]
27. Chen, S.; Zhang, Y.; Wu, Q.; Gao, H.; Yan, D. Residual Stress Relief for 2219 Aluminum Alloy Weldments: A Comparative Study on Three Stress Relief Methods. *Metals* **2019**, *9*, 419. [CrossRef]
28. Song, H.; Gao, H.; Wu, Q.; Zhang, Y. Effects of Segmented Thermal-Vibration Stress Relief Process on Residual Stresses, Mechanical Properties and Microstructures of Large 2219 Al Alloy Rings. *J. Alloys Compd.* **2021**, *886*, 161269. [CrossRef]
29. Li, B.; Dong, Y.; Gao, H. Numerical Simulation and Experiment of Stress Relief and Processing Deformation of 2219 Aluminum Alloy Ring. *Metals* **2023**, *13*, 1187. [CrossRef]
30. Gao, H.; Li, X.; Li, B.; Wu, Q.; Ma, Y.; Jian, X.; Chen, S. Residual Stress and Microstructure of Ti6Al4V Treated by Thermal-Vibratory Stress Relief Process. *J. Mater. Res. Technol.* **2022**, *18*, 5161–5181. [CrossRef]
31. Gao, Z.; Zhang, Y.; Gao, H.; Wu, Q. Experimental Study and Simulation Analysis of Thermal-Vibratory Stress Relief Treatment of Al-Cu-Mg Alloy Plate. *J. Manuf. Process.* **2023**, *92*, 124–134. [CrossRef]
32. Morris, C.; Zhang, L.; Green, R. Thermal Residual Stresses in Co-Continuous Composites: Recent Advances. *Acta Mater.* **2024**, *239*, 118133.
33. Gao, L.; Sun, X.; Wang, Q. A Mechanics Model for Thermal Residual Stresses in Metal Matrix Composites. *J. Mater. Sci. Technol.* **2023**, *99*, 72–82.
34. Balokhonov, R.; Kulkov, A.; Zemlyanov, A.; Romanova, V.; Evtushenko, E.; Gatiyatullina, D.; Kulkov, S. Evolution of Residual Stresses and Fracture in Thermomechanically Loaded Particle-Reinforced Metal Matrix Composites. *Phys. Mesomech.* **2021**, *24*, 503–512. [CrossRef]
35. Zhang, X.; Xiao, B.; Andrä, H.; Ma, Z. Multi-Scale Modeling of the Macroscopic, Elastic Mismatch and Thermal Misfit Stresses in Metal Matrix Composite. *Compos. Struct.* **2015**, *125*, 176–187. [CrossRef]

36. Gao, Z.; Gao, H.; Zhang, Y.; Wu, Q. Experiment and Mechanism Investigation on The Effect of Heat Treatment on Residual Stress and Mechanical Properties of SiCp/Al–Cu–Mg Composites. *Mater. Sci. Eng. A* **2023**, *884*, 145555. [CrossRef]
37. Zhao, Y.; Liu, Y.; Zhang, J.; Yang, H. Thermal Expansion and Stability of Al–Si Matrix Composites Reinforced with High-Content SiC. *J. Mater. Sci. Technol.* **2023**, *97*, 186–195.
38. Zhang, T.; Li, J.; Zhou, M. Advanced SiC/Al Composites for Aerospace Applications: Performance and Innovations. *Aerosp. Sci. Technol.* **2023**, *130*, 107560.
39. Chen, L.; Zhang, Y.; Liu, Q. High-Temperature Creep Behavior of SiC Fiber-Reinforced Ceramic Matrix Composites. *Mater. Manuf. Process.* **2023**, *38*, 1287–1298.